ISSN 1330–0008
CODEN FIZAE4

IONIZATION OF ATOMS IN ENCOUNTER WITH ATOMIC PROJECTILES

R. DAS, S. SAHOO[1] and K. ROY

Department of Theoretical Physics, Indian Association for the Cultivation of Science, Jadavpur, Calcutta 700 032, INDIA
E-mail: tprd@mahendra.iacs.res.in

Received 12 December 2000; revised manuscript received 22 June 2001
Accepted 5 September 2001

Ionization of mono-electron and multi-electron target atoms has been studied at different impact energies ranging from 5 to 1000 keV using Born approximation. Total cross-sections for the ionization of H, He and Ne in collision with atomic projectiles such as H and He are reported. For the bound state wave functions of He and Ne, simplifications are made by assuming that the atom has single active electron and is influenced by an effective potential due to the passive electrons and the residual core. We represent the bound state wave functions by Slater type orbitals obtained from the model potential. In the final channel, we consider the continuum state wave function is centered around the ionized site of the target atom. The results thus obtained are compared with other theoretical predictions as well as with experimental data. On comparing, reasonably good agreements have been found in the intermediate and high energy region.

PACS numbers: 34.10.+x, 34.90.+q UDC 537.563.3

Keywords: Ionization, bound state wave function, continuum state wave function, multi-electron target atoms, Slater type orbitals, model potential

1. Introduction

A significant progress has been made to study the direct ionization i.e. the ejection of an electron in an atom–atom collisional system. Reactions involving neutral atoms in their ground states play an important role in plasma, fusion and many other astrophysical processes. It is, therefore, needed to calculate the ionization cross-sections for both slow and fast collisions to a greater accuracy.

For the single ionization of atoms by impact of fully stripped ions, many theoretical and experimental works have been carried out so far. The process does not

[1]Present address: Institute of Material Science, Univ. of Tsukuba, Ibaraki 305-8573, JAPAN

involve much complexity as the projectile is capable of removing single electron from the target atoms only. However, collision involving projectile having structure (i.e. having one or more bound electrons with it) is considerably more complex to treat theoretically. In these collisions, it may be possible that the projectile electrons undergo excitation and ionization, and these are not necessarily accompanied by target excitation or ionization. An additional theoretical problem arises when the target atoms partially or fully screen the projectile nuclear charge, and this screening depends on the impact parameter values of the corresponding collisions.

Bates and Griffing [1] investigated theoretically the ionization and excitation processes involving H–H collisions in the high-energy region. They reported the total ionization cross-section values for the above reactions. In 1968, McClure [2] measured the cross-sections for the electron loss and electron capture by the hydrogen atom when it encounters with H atom targets in the energy range of 1.25 to 117 keV. He reported that the theoretical cross-section values obtained by Bates and Griffing [1] for ionization process are by about a factor of 2 smaller than his experimental data at 20 keV, and the values are nearly equal between 80 to 100 keV. Excitation and ionization cross-sections in collisions between ground states of hydrogen atoms have been studied by Shingal et al. [3] using a coupled channel method taking 22-state basis around each heavy particle. In 1996, Krstic et al. [4] studied the single ionization of hydrogen atom by impact of hydrogen in the low energy region of 50 eV to 4 keV. They have used the hidden crossing method which is generalized to treat multielectron system using molecular Hartree-Fock and configuration interaction methods. Riley and Ritchie [5] calculated the ionization cross-section for the H+H system in the intermediate energy region where most of the inelastic processes occur by solving the Schrödinger equation in space and time and assuming one of the electrons is frozen in the 1s state. In a very recent work [6], these authors have studied the excitation and ionization in H–H collision, solving numerically the coupled three-dimensional Schrödinger equation for the two electron orbitals in singlet and triplet symmetries.

Bell et al. [7] studied the ionization of helium by hydrogen atom impact using simple Born approximation. They have used the many-parameter correlated wave functions in their calculation. The experimental data on the ionization cross-sections were obtained by DuBois and Kover [8] in the range 25-1000 keV/amu for single and double ionization of helium by impact of hydrogen. The values above 200 keV were of good agreement as compared to the results of Bell et al. [7].

In the present work, we restrict ourselves to calculate the total ionization cross-sections of hydrogen, helium and neon by impact of hydrogen and helium in the intermediate to high energy region, in the first Born approximation, taking proper account of the electron-electron interactions.

2. *Theory*

The collision system in the present study is a complex one due to the presence of more than one electron in the target atoms except hydrogen atom. In order to simplify it, we treat the multi-electron target atoms as having only one active electron, which experiences an effective potential due to the residual target core and the passive electron(s). We solve the one-electron Schrödinger equation for the system with electronic Hamiltonian

$$H_e = -\frac{1}{2}\nabla_r^2 + V_T(r_2) + V_p(r_1) + \frac{1}{r_{12}} \tag{1}$$

(atomic units are used throughout), where $\vec{r_2}(\vec{r_1})$ is the distance of the electron corresponding to the nuclei of target (projectile) and $\vec{r}_{12}$ is the distance between the two electrons. We adopt here the impact parameter formalism, where the internuclear motion is treated classically as $\vec{R} = \vec{p} + \vec{v}t$, in which $\vec{p}$ is the impact parameter and $\vec{v}$ the relative velocity of the projectile with the target. Time t is measured from the instant when the two nuclei are closest to each other, i.e., at that point t is to be considered to be zero.

The development in time t of the transition amplitude for ionization with the ejection of an electron with momentum $\vec{k}$ can be written as

$$\frac{\mathrm{d}}{\mathrm{d}t}(c_k(p)) = \int [\Psi_f^{-\star}(H_e - \mathrm{i}\frac{\mathrm{d}}{\mathrm{d}t})\Psi_i]\mathrm{d}\vec{r}, \tag{2}$$

with the initial condition that at $t = -\infty, c_k = 0$. The ionization probability is $|c_k(t = +\infty)|^2$.

We consider the continuum state wave function is centered around the ionized state of target and it takes the form

$$\Psi_{k_c} = \frac{N_T}{(2\pi)^{\frac{3}{2}}} \mathrm{e}^{\mathrm{i}\vec{k}\cdot\vec{r_2}} {}_1F_1(\mathrm{i}\alpha_T, 1; -\mathrm{i}(k_T r_2 + \vec{k_T} \cdot \vec{r_2})) \times \mathrm{e}^{-\mathrm{i}k^2 t/2}, \tag{3}$$

where $\alpha_T = -q_T/k_T$, $\vec{k_T} = \vec{k} + \vec{v}/2$, and $N_T = \mathrm{e}^{-\pi\alpha_T/2}\Gamma(1 + \mathrm{i}\alpha_T)$, q_T is the asymptotic charge of the target ion. Now we can write the final state wave function

$$\Psi_f^- = \phi_i(r_1)\exp(\frac{\mathrm{i}}{2}\vec{v}\cdot\vec{r_1})\exp((-\mathrm{i}\epsilon_1 - \frac{\mathrm{i}}{8}v^2)t) \times \Psi_{k_c}, \tag{4}$$

where $\phi_i(r_1)$ is the electronic wave function of the projectile in its bound state which is described in Sect. 2.1.

When we consider the projectile ionization, we take the continuum state wave function around the projectiles of the form

$$\Psi_{k_c} = \frac{N_p}{(2\pi)^{\frac{3}{2}}} \mathrm{e}^{\mathrm{i}\vec{k}\cdot\vec{r_1}} {}_1F_1(\mathrm{i}\alpha_p, 1; -\mathrm{i}(k_p r_1 + \vec{k_p} \cdot \vec{r_1})) \times \mathrm{e}^{-\mathrm{i}k^2 t/2}, \tag{5}$$

where $\alpha_p = -Z_p/k_p$, $\vec{k_p} = \vec{k} - \vec{v}/2$, and $N_p = \mathrm{e}^{-\pi\alpha_p/2}\Gamma(1+\mathrm{i}\alpha_p)$, Z_p is the asymptotic charge of the projectile ion. Now we can write the final state wave function

$$\Psi_f^- = \phi_i(r_2)\exp(\frac{\mathrm{i}}{2}\vec{v}\cdot\vec{r_2})\exp((-\mathrm{i}\epsilon_2 - \frac{\mathrm{i}}{8}v^2)t) \times \Psi_{k_c}\,, \tag{6}$$

where $\phi_i(r_2)$ is the electronic wave function of the target in its bound state which is described in Sect. 2.1.

The above final-state wave function asymptotically satisfies the Schrödinger equation,

$$(-\frac{1}{2}\nabla_r^2 - \frac{Z_T}{r_2} - \frac{Z_p}{r_1} + \frac{1}{r_{12}} - \mathrm{i}\frac{\partial}{\partial t})\Psi_f^- = 0\,, \tag{7}$$

where Z_p is the nuclear charge of the projectile.

2.1. Construction of initial bound-state wave function

The interaction of active electron and the residual target ion of asymptotic charge q_T may be described in different ways. We have used a model potential of the form

$$V_T = -\frac{q_T}{r_2} - \frac{\exp(-\lambda r_2)}{r_2}\{(Z - q_T) + br_2\}\,, \tag{8}$$

where Z is the nuclear charge of the target ion.

This model potential contains two parts, first part represents the long-range Coulomb potential and the second part represents the short-range potential. When we treat the multi-electron target atom as one electron atom, the other electrons make a core with the nuclei, there the distortion, correlation and other effects are present. These are represented by the short-range part of the model potential and the effective (excited) electron effect is represented by the long-range part of this potential. So the bound-state wave functions of multi-electron target atoms are represented by Slater type orbitals obtained from this model potential and have reported encouraging results. In the present case, the arbitrary parameters, b and λ are chosen variationally with respect to Slater basis set in such a way that the corresponding Hamiltonian of the active electron is diagonalized to reproduce correct binding energy. The binding energy of the active electron on target ion is calculated from the tables of Clementi and Roetti [9]. To check the accuracy of the wave function, virial theorem has been tested, and is found to be accurate within 0.01%. The present model potential is similar to those used by Ermolaev et al. [10] and Ermolaev [11] in their studies on charge transfer processes involving lithium and cesium targets and also used by Sahoo et al. [12] in the study of ionization of multi-electron atoms.

The initial state wave function used in the present approach can be written as

$$\begin{aligned}\Psi_i \quad &= \quad \phi_i(r_1)\phi_i(r_2)\exp\left(\frac{\mathrm{i}}{2}\vec{v}\cdot\vec{r_1}\right)\,\exp\left(\left(-\mathrm{i}\epsilon_1 - \frac{\mathrm{i}}{8}v^2\right)t\right)\\ &\quad\times\exp\left(-\frac{\mathrm{i}}{2}\vec{v}\cdot\vec{r_2}\right)\,\exp\left(\left(-\mathrm{i}\epsilon_2 - \frac{\mathrm{i}}{8}v^2\right)t\right),\end{aligned} \tag{9}$$

with $\phi_i(r_1)=\sum_j c_j^{nl}\exp(-\beta_j r_1)r_1^l Y_{lm}(\hat{r}_1)$ and $\phi_i(r_2) = \sum_j c_j^{nl}\exp(-\beta_j r_2)r_2^l Y_{lm}(\hat{r}_2)$, c_j and β_j are the coefficients and the exponents of the Slater orbitals.

2.2. Transition amplitude

The transition amplitude as shown in Eq. (2) may be derived in the following ways. Using Eqs. (4), (7) and (9), we may write Eq. (2) as

$$\begin{aligned} c_k(p) &= A_k \int \mathrm{e}^{\mathrm{i}Et} \mathrm{d}t \int \mathrm{e}^{-2\lambda r_1} \mathrm{e}^{-\lambda r_2} \mathrm{e}^{-\mathrm{i}\vec{K}\cdot\vec{r_2}} \; {}_1F_1(-\mathrm{i}\alpha_T, 1; \mathrm{i}(k_T r_2 + \vec{k_T}\cdot\vec{r_2})) \\ & \times \left[-\frac{1}{|R+r_1|} - \frac{1}{|R-r_2|} + \frac{1}{|R+r_1-r_2|} \right] \mathrm{d}\vec{r_1} \mathrm{d}\vec{r_2} \,, \end{aligned} \tag{10}$$

where $\vec{K} = \vec{k} + \vec{v}/2, E = k^2/2 - v^2/8 - \epsilon_2$ and $A_k = (N_T^\star/\pi\sqrt{\pi})(\lambda^3/(2\pi)^{3/2}$. To evaluate Eq. (10), let us first integrate the following

$$\begin{aligned} J &= \int \mathrm{e}^{-\mu r_1} \mathrm{e}^{-\lambda r_2} \mathrm{e}^{-\mathrm{i}\vec{K}\cdot\vec{r_2}} \; {}_1F_1(-\mathrm{i}\alpha_T, 1; \mathrm{i}(k_T r_2 + \vec{k_T}\cdot\vec{r_2})) \\ & \times \left[-\frac{1}{|R+r_1|} - \frac{1}{|R-r_2|} + \frac{1}{|R+r_1-r_2|} \right] \mathrm{d}\vec{r_1} \mathrm{d}\vec{r_2} \,, \end{aligned} \tag{11}$$

where $\mu = 2\lambda$. The above integral in Eq. (11) is consisting of three independent integrals defined as below,

$$A = -\int \mathrm{e}^{-\mathrm{i}\vec{K}\cdot\vec{r_2}} \mathrm{e}^{-\lambda r_2} \frac{\mathrm{e}^{-\mu r_1}}{|R+r_1|} \times {}_1F_1(-\mathrm{i}\alpha_T, 1; \mathrm{i}(k_T r_2 + \vec{k_T}\cdot\vec{r_2})) \mathrm{d}\vec{r_1} \mathrm{d}\vec{r_2} \,, \tag{12}$$

$$B = -\int \mathrm{e}^{-\mathrm{i}\vec{K}\cdot\vec{r_2}} \mathrm{e}^{-\lambda r_2} \frac{e^{-\mu r_1}}{|R-r_2|} \times {}_1F_1(-\mathrm{i}\alpha_T, 1; \mathrm{i}(k_T r_2 + \vec{k_T}\cdot\vec{r_2})) \mathrm{d}\vec{r_1} \mathrm{d}\vec{r_2} \,, \tag{13}$$

and

$$C = \int \mathrm{e}^{-\mathrm{i}\vec{K}\cdot\vec{r_2}} \mathrm{e}^{-\lambda r_2} \frac{\mathrm{e}^{-\mu r_1}}{|R+r_1-r_2|} \times {}_1F_1(-\mathrm{i}\alpha_T, 1; \mathrm{i}(k_T r_2 + \vec{k_T}\cdot\vec{r_2})) \mathrm{d}\vec{r_1} \mathrm{d}\vec{r_2} \,. \tag{14}$$

On performing the integration over $\vec{r_1}$ and $\vec{r_2}$, Eq. (12) may be written as

$$A = -\frac{8\pi^2}{T^2} \phi^{-\mathrm{i}\alpha_T} \left[\frac{1}{R} - \left(1 + \frac{1}{R}\right) \mathrm{e}^{-2R} \right] \times \left[1 + \mathrm{i}\alpha_T \left(\frac{1 - \mathrm{i}k_T}{\phi} - 1 \right) \right] , \tag{15}$$

where $\phi = (v^2/4 - k_T^2 + \lambda^2 - 2\mathrm{i}\lambda k_T)/T$ and $T = \lambda^2 + K^2$. Similarly, on integrating Eq. (13) and Eq. (14) over $\vec{r_1}$, we may write

$$B = -\frac{8\pi}{\mu^3} \int \frac{\mathrm{e}^{-\mathrm{i}\vec{K}\cdot\vec{r_2}} e^{-\lambda r_2}}{|R-r_2|} \times {}_1F_1(-\mathrm{i}\alpha_T, 1; \mathrm{i}(k_T r_2 + \vec{k_T}\cdot\vec{r_2})) \mathrm{d}\vec{r_2} \,, \tag{16}$$

and

$$C = \frac{8\pi}{\mu^3}\int \frac{\mathrm{e}^{-\mathrm{i}\vec{K}\cdot\vec{r_2}}e^{-\lambda r_2}}{|R-r_2|}\ {}_1F_1(-\mathrm{i}\alpha_T, 1; \mathrm{i}(k_T r_2 + \vec{k_T}\cdot\vec{r_2}))\mathrm{d}\vec{r_2} + \frac{\partial}{\partial\mu}(\frac{4\pi}{\mu^2})\int \mathrm{e}^{-\mathrm{i}\vec{K}\cdot\vec{r_2}}e^{-\lambda r_2}\frac{e^{-\mu|R-r_2|}}{|R-r_2|}\ {}_1F_1(-\mathrm{i}\alpha_T, 1; \mathrm{i}(k_T r_2 + \vec{k_T}\cdot\vec{r_2}))\mathrm{d}\vec{r_2}. \tag{17}$$

The integral in Eq. (17) is a linear combination of two separate integrals which may be denoted as C_1 and C_2, respectively.

It may be seen that one of the terms of the integral C in Eq. (17) cancels with the integral B in Eq. (16), and hence we get $J = A + C_2$.

Using Fourier transformation technique and performing contour integration over t_1, we get

$$C_2 = -8Lt_{\mu\to 2}Lt_{\lambda\to 1}\left(\frac{\partial^2}{\partial\mu\partial\lambda}\right)\left(\frac{1}{\mu^2}\right)\int \frac{\mathrm{e}^{\mathrm{i}\vec{Q}\cdot\vec{R}}}{(Q^2+\mu^2)}\mathrm{d}Q\ A_1^{(-1-\mathrm{i}\alpha_T)}(A_1 - B_1)^{\mathrm{i}\alpha_T}, \tag{18}$$

where $A_1 = (\vec{Q}+\vec{K})^2 + \lambda^2$ and $B_1 = 2[\vec{k_T}\cdot(\vec{Q}+\vec{K}) + \mathrm{i}\lambda k_T]$.

Finally, we may write Eq. (2) as $c_k(p) = A_k\int \mathrm{e}^{\mathrm{i}Et}\mathrm{d}t(A + C_2)$. Now, $c_k(p)$ may be written as a sum of two different integrals as follows

$$c_k(p) = A_k\int \mathrm{e}^{\mathrm{i}Et}A\mathrm{d}t + A_k\int \mathrm{e}^{\mathrm{i}Et}C_2\mathrm{d}t\,. \tag{19}$$

The first integral in Eq. (18) is solved analytically by using Bessel function [13] and the second integral is evaluated numerically following the procedures adopted in Ref. [12].

The doubly differential cross-sections may be written as $\frac{\mathrm{d}^2\sigma}{\mathrm{d}E_e\mathrm{d}\Omega_e} \approx k\int \mathrm{d}^2p|c_k(p)|^2$ and the total ionization cross-sections (σ_{total}) are calculated by using the following integral, $\sigma_{\mathrm{total}} = 2\pi\int \frac{\mathrm{d}^2\sigma}{\mathrm{d}E_e\mathrm{d}\Omega_e}\sin\theta_e\mathrm{d}\theta_e\mathrm{d}E_e$. (Symbols have their usual meanings.)

For the case of projectile ionization, similar procedure can be made considering the appropriate wave functions.

3. Results and discussion

We have calculated the total ionization cross-sections of the following reactions:

$$\begin{array}{rlcl}
(i) & \mathrm{H_P}+\mathrm{H_T} & \to & \mathrm{H_P}+\mathrm{H_T^+}+\mathrm{e} \\
(ii) & \mathrm{H_P}+\mathrm{H_T} & \to & \mathrm{H_P^+}+\mathrm{H_T}+\mathrm{e} \\
(iii) & \mathrm{H_P}+\mathrm{He_T} & \to & \mathrm{H_P}+\mathrm{He_T^+}+\mathrm{e} \\
(iv) & \mathrm{He_P}+\mathrm{H_T} & \to & \mathrm{He_P}+\mathrm{H_T^+}+\mathrm{e} \\
(v) & \mathrm{H_P}+\mathrm{Ne_T} & \to & \mathrm{H_P}+\mathrm{Ne_T^+}+\mathrm{e}
\end{array}$$

(Subscripts P and T denote the projectile and target, respectively.)

In these reactions, both projectile and target are neutral atoms and either projectile or target is ionized in the final channel.

In Fig. 1, the values of cross-sections for target ionization in the reaction (i) are presented. On comparison with other theoretical results as well as with the experimental data, it is found that the present results are in good agreement with the experimental data of McClure [2] in the energy range of 6 keV to 40 keV. The theoretical values of Shingal et al. [3], who made calculations with Born corrections, are found to be a little higher than the present results for 20 keV incident energy. Above this energy region, though the present results are of higher magnitude, they are closer to the experimental data [2]. The values calculated by Riley and Ritchie [5] with frozen core approximation are found to be of smaller magnitude in comparison with the present results above 9 keV impact energy, and below this energy region the present results are found to be smaller in magnitude compared to Riley and Ritchie [5]. However, the present results show a qualitative agreement with all theoretical values and experimental data presented in the figure. In Ref. [5], the time dependent Schrödinger equation with an effective Hamiltonian was solved, where in the effective interaction was obtained by averaging over a frozen core model and also one electron approximation was considered. We have used the Born approximation considering the two-electron approximation, and the interaction is taken without any averaging. The very recent results of Riley and Ritchie [6]

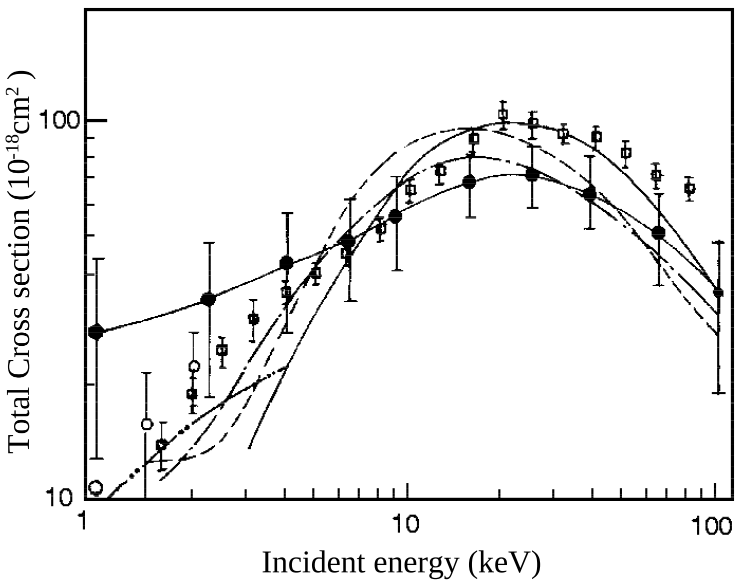

Fig. 1. Total ionization cross-sections for the system in reaction (i). Present results: solid line, Shingal et al. (Ref. [3]): dashed line, Riley and Ritchie (Ref. [5]): dashed dot line, Riley and Ritchie (Ref. [6]): solid line with closed circle, Krstic et al. (Ref. [4]): dashed double dot line. Experimental data: McClure (Ref. [2]): open square, Gealy and Van Zyl (Ref. [13]): open circle.

obtained by solving the coupled three-dimensional Schrödinger equations for two electron orbitals in singlet and triplet symmetries are also found to be smaller in magnitude in comparison to the present results in the intermediate energy range. In the low energy region, the present results fall off rapidly in comparison to the results of Ref. [6]. Better performance of the present method at higher energies may be due to the validity of the Born approximation in this energy region. However, in the low impact energy region, the present results fail to reproduce the other available theoretical as well as experimental data. In the low energy region, Krstic et al. [4] studied the ionization cross-section of H by impact of H by using hidden crossing method and predicted better results in comparison with other available experimental and theoretical results. The results of Ref. [4] are much higher below 4 keV than the present results. The present results are also found to be smaller in magnitude in comparison with the experimental data of Gealy and Van Zyl [14] in the low energy region. This discrepancy arises due to the fact that the present method gives better results only in the high-energy region.

Figure 2 displays the values of the total ionization cross-sections for the system in reactions (i) and (ii). Since the reactions are symmetric, it may be seen from the figure that the cross-section values for projectile ionization are of the same magnitude in comparison with the values for target ionization. We have also displayed in the same figure the total cross-sections for H–H system obtained from simple addition of the cross-sectional values due to projectile and target ionization.

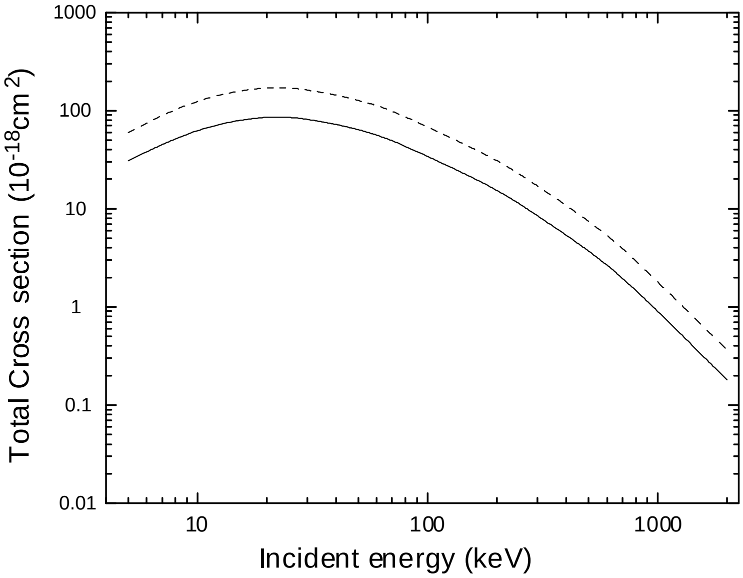

Fig. 2. Total ionization cross-sections for both target and projectile ionization for the reactions (i) and (ii). Solid line represents the present results for both projectile ionization and target ionization which coincide and dashed line shows the present results after adding both the above cross-sections.

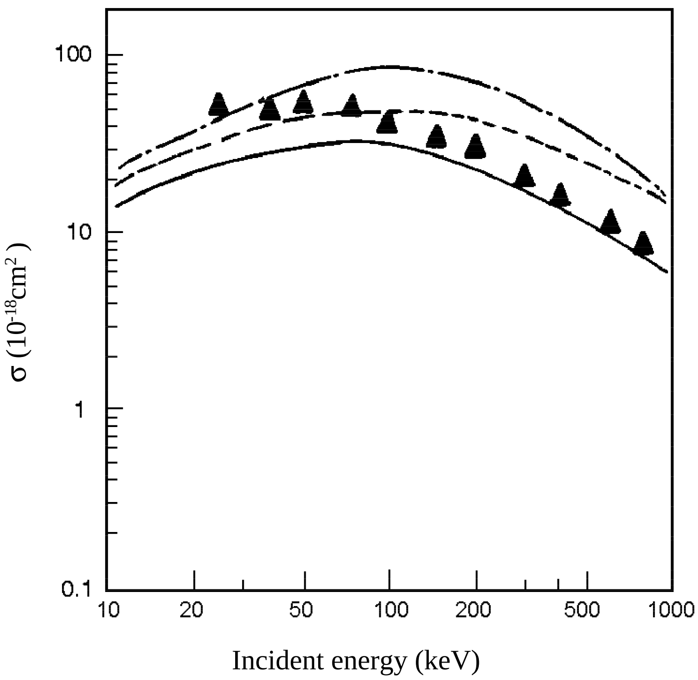

Fig. 3. Total ionization cross-sections of He *by* H *impact as a function of collision energy. Theory: Present results: solid line, Born results (Ref. [7]): dashed line, experimental data (Ref. [8]): solid triangle. Total cross-sections of* He *by* H^+ *impact as a collision impact energy (Ref. [11]): dashed dot line.*

In Fig. 3, we present the total ionization cross-sections of helium atom by neutral hydrogen impact as shown in the reaction (iii) in the energy range between 10 to 1000 keV. For comparison, other theoretical values as well as the experimental data have also been presented in the same figure. The present results are found to be in a reasonably good agreement with the experimental data of DuBois and Kover [8] above 90 keV impact energy. The Born results of Bell et al. [7] are found to be higher in magnitude in comparison with the present values as well as the experimental data [8] throughout the energy range considered.

In the same figure we have also presented the previously calculated values for proton impact ionization of He atom [12]. It is evident from the figure that the results for proton impact ionization are around three times higher in magnitude than those calculated for hydrogen impact ionization of He. This is due to the fact that in the case of hydrogen atom impact on helium, there is bound electron effect of the projectile and also the electron-electron interaction effects arise which reduce the cross-sections for atom impact compared to the case for ion impact throughout the energy region. Here it may be pointed out that in the Ref. [12], we have used the same Slater type wave functions as in the present work.

Figure 4 presents the total ionization cross-sections for the target ionization in reactions (iii) and (iv). It may be seen that the values for the projectile ionization in reaction (iii) are higher in magnitude in comparison with the values for target ionization in reaction (iv) and the ratio is around 2.72 at 100 keV. We also display in the same figure the total cross-section for H-He system derived from simple addition of the cross-sections due to projectile and target ionization.

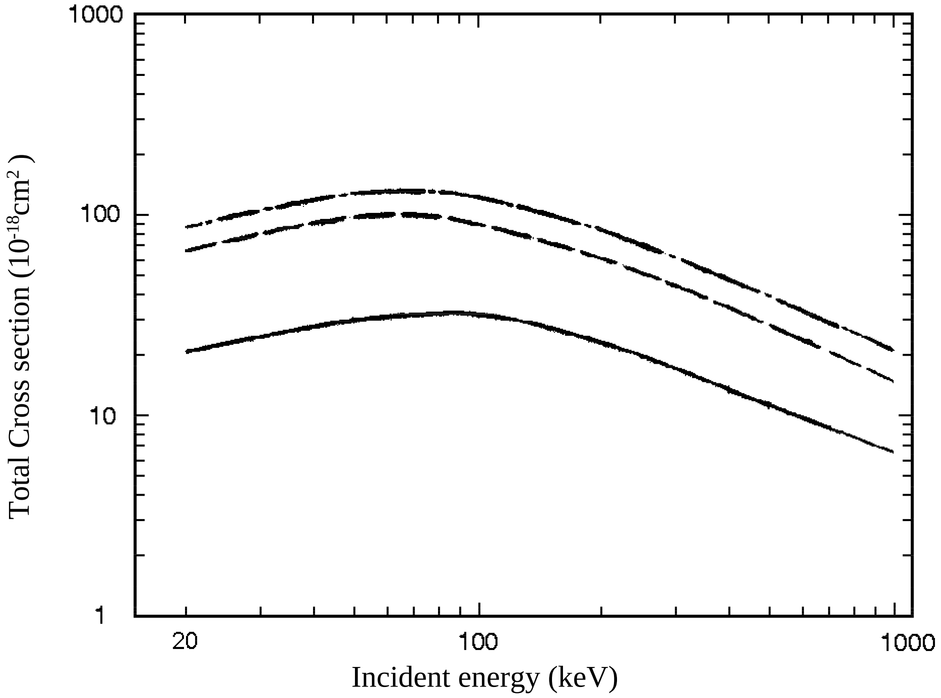

Fig. 4. Total ionization cross-sections for reaction (iii) and (iv). Present results: target ionization: solid line, projectile ionization: dashed line and linear combination of cross-sections for both the above reactions (iii) and (iv): dashed dot line.

Figure 5 displays the total ionization cross-section values for the reaction (v). For comparison, we have presented the cross-section value for proton impact ionization of Ne [15,16]. It is found from the figure that the cross-section values for reaction in (v) lie well below the results the p-Ne result throughout the energy range considered. It is also evident from the figure that the cross-section values for p-Ne system [16] are found to be 11.8 times larger than those obtained in the reaction (v) at 100 keV/amu and about 9 times larger at 1000 keV. We have made a comparison of the present results for proton impact ionization of Ne with the experimental data of Afrosimov et al. [15] and a very good agreement has been achieved. It may be noted that the results for p-Ne system and a detailed comparison with other available theoretical values and experimental data for the same system will appear in our next paper [16].

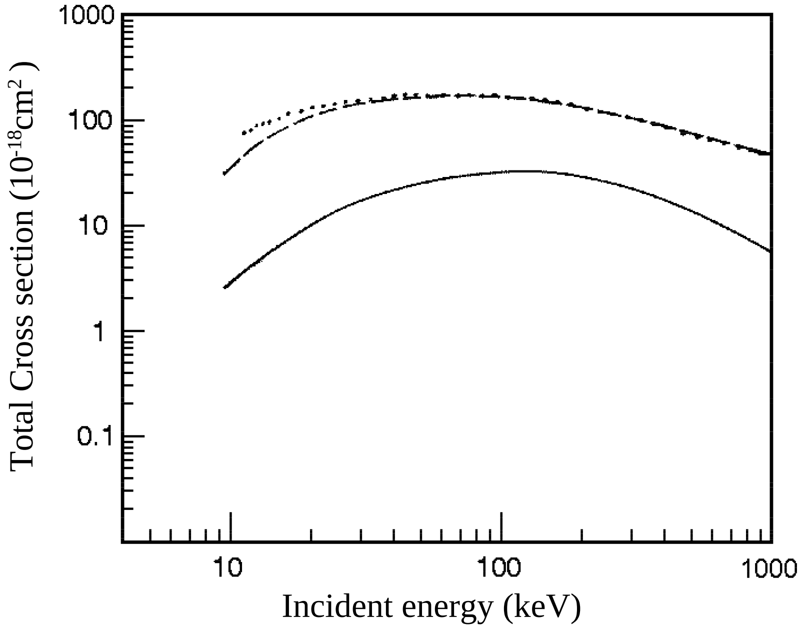

Fig. 5. Total ionization cross-sections for reaction (v). Present results: solid line. Total ionization cross-sections of Ne *by* H^+ *impact: (Ref. [16]): dashed line, experimental data (Ref. [14]): doted line.*

4. Conclusion

We have reported the total ionization cross-sections for atom-atom collisions. The results obtained are found to be in reasonably good accord with the available theoretical findings as well as with the experimental data. The present results for the multi-electron target-atom collisions are found to be encouraging in the sense that we have used Slater type wave function obtained from the model potential instead of correlated wave function.

The present theoretical approach is comparatively simpler and easier to tackle numerically. Fairly good results can be predicted for systems involving many electrons in the intermediate and high energy regions.

Acknowledgements

The authors greatly acknowledge valuable comments and suggestions of Prof. S. C. Mukherjee and Prof. N. C. Sil.

References

[1] D. R. Bates and G. Griffing, Proc. Phys. Soc. A **66** (1953) 961.

[2] G. W. McClure, Phys. Rev. **166** (1968) 22.

[3] R. Shingal, B. H. Bransden and D. R. Flower, J. Phys. B **22** (1989) 855.

[4] P. S. Krstic, G. Bent and D. R. Schultz, Phys. Rev. lett. **77** (1996) 2428.

[5] M. E. Riley and A. B. Ritchie, J. Phys. B **32** (1999) 5279.

[6] M. E. Riley and A. B. Ritchie, J. Phys. B **33** (2000) 5177.

[7] K. L Bell, V. Dose and A. K. Kingston, J. Phys. B **2** (1969) 831.

[8] R. D. DuBois and A. Kover, Phys. Rev. A **40** (1989) 3605.

[9] E. Clementi and C. Roetti, At. Data Nucl. Data Tables **14** (1974) 177.

[10] A. M. Ermolaev, C. J. Noble and B. H. Bransden, J. Phys. B **15** (1982) 457.

[11] A. M. Ermolaev, J. Phys. B **17** (1984) 1069.

[12] S. Sahoo, R. Das, N. C. Sil, S. C. Mukherjee and K. Roy, Phys. Rev. A **62** (2000) 022716.

[13] G. N. Watson, *Treatise on the Theory of Bessel Functions*, 2nd ed., Cambridge Univ. Press, Cambridge (1944).

[14] M. W. Gealy and B. Van Zyl, Phys. Rev. A **36** (1987) 3100.

[15] V. V. Afrosimov, Yu. A. Mamaev, M. N. Panov and N. V. Federenko, Zh. Tekh. Fiz. **39** (1969) 159 [Sov. Phys. Tech. Phys. **14** (1969) 109].

[16] R. Das, S. Sahoo and K. Roy, to be published.

IONIZACIJA ATOMA SUDARIMA S ATOMSKIM PROJEKTILIMA

Proučavali smo ionizaciju jedno i višeelektronskih atoma meta za više upadnih energija od 5 do 1000 keV primjenom Bornovog približenja. Dajemo ukupne udarne presjeke za ionizaciju H, He i Ne u sudarima s atomskim projektilima H i He. Valne funkcije He i Ne smo pojednostavnili pretpostavljajući da atom ima jedan aktivan elektron a na njega djeluje efektivni potencijal jezgre i pasivnih elektrona. Valne funkcije vezanih stanja predstavljamo orbitalama Slaterovog tipa iz modelnog potencijala. U konačnom stanju razmatramo valnu funkciju kontinuuma kojoj je središte oko ioniziranog stanja atoma mete. Postignuti ishodi računa usporeduju se s predvidanjima drugih autora i s eksperimentalnim podacima. Postigli smo razumno dobro slaganje u srednjem i višem energijskom području.